Japan Geoscience Union Meeting 2015
(May 24th - 28th at Makuhari, Chiba, Japan)

SVC46-P01 Room:Convention Hall Time:May 25 18:15-19:30

Experimental simulation of mixing processes of crystal-rich and -free magmas

KOMAMIYA, Chizen[1*] ; OKUMURA, Satoshi[1] ; NAKAMURA, Michihiko[1]

[1]Department of Earth Science, Graduate School of Science, Tohoku University

Volcanic and plutonic rocks often show textural and petrological evidence on mixing of magmas with different chemical composition and temperature. Several experimental studies have been performed to reproduce textures found in natural rocks and to reveal the mechanism of magma mixing (e.g., Kouchi and Sunagawa, 1982; De Campos et al., 2008, 2011; Laumonier et al., 2014). Important processes that control magma mixing are crystallization and melting of crystals in magmas because they strongly change magma viscosity (Laumonier et al., 2014). For example, when magmas with different temperature contact and mix, crystallization and melting of crystals which are induced by thermal interaction are expected to occur in a hotter magma and in a colder magma, respectively. In addition, the crystallization in a hotter magma is enhanced by shear flow (e.g., Vona and Romano, 2013).

In this study, we experimentally simulated mixing processes of crystal-rich and -free magmas by using an image furnace. In experiments, crystal-rich rock samples with ~5 mm in an outer diameter (trachyandesite lava from Rishiri volcano and dacite lava from Unzen volcano) were contacted with a crystal-free glass, and then the samples were heated and twisted in the furnace. We used a glass sample synthesized from alkaline rock (trachyandesite lava) because it has relatively low viscosity even at 1 bar under dry conditions. The mixing experiments in the furnace were performed at a temperature of ca. 1100 ℃ (hot spot) under a shear rate of 4.2×10^{-2} s^{-1}. The samples were twisted for 6, 30, and 60 minutes. Because the glass sample synthesized at a temperature of 1400 ℃ is an undercooled melt at experimental temperature (1100 ℃), the crystallization of the melt is expected to occur, and this simulates cooling and crystallization of a hotter magma during magma mixing. After experiments, quenched run products were observed using optical and scanning electron microscopes.

In mixing experiments of the trachyandesite rock and the glass sample, the melting of crystals in crystal-rich magma was observed, while plagioclase crystallizes in crystal-free melt at the boundary of crystal-rich and -free magmas. The mingling between crystal-rich and -free magmas started to be found after 30 min. The mingling seems to enhance the crystallization in crystal-free magma. In a run product of a 60 min experiment, the part of originally crystal-free magma was highly crystallized. The experimental results indicate that the mingling between crystal-rich and -free magmas starts when melt fraction in the crystal-rich magma is high enough to cause the mingling, and it enhances the crystallization of originally crystal-poor magma, which results in rapid increase of magma viscosity. In contrast, the mingling was found only at a 60 min experiment for mixing experiments of the dacite rock and the glass sample. This difference between trachyandesite and dacite rocks may indicate that the onset of the mingling is controlled by the combination of crystal content in crystal-rich magma and the viscosity ratio of melt phases. Our experiments imply that the coupled effect of crystallinity change and mingling controls the mixing of magmas with originally different crystallinity, that is, different chemical composition and temperature.

Keywords: Magma mixing, Magma mingling, Shear flow, Crystallization, Viscosity

Japan Geoscience Union Meeting 2015
(May 24th - 28th at Makuhari, Chiba, Japan)

SVC46-P02 Room:Convention Hall Time:May 25 18:15-19:30

Pre-eruptive conditions and eruptive process of the Tsurumi-dake summit lava; constraints from hornblende phenocrysts

NAGASAKI, Shiho[2] ; ISHIBASHI, Hidemi[1*] ; TAKEMURA, Keiji[3]

[1]Grauate School of Science, Shizuoka University, [2]Faculty of Science, Shizuoka University, [3]Graduate School of Science, Kyoto University

Textural and chemical analyses were done for hornblende phenocrysts in Tsurumi-dake summit lava to constrain its pre-eruptive conditions and eruption processes. Tsurumi-dake summit lava, the latest lava erupted at 7.3-10.5ka (Fujisawa et al., 2002), is andesitic with ca. 30 vol.% of phenocrysts consisting of plagioclase, hornblende, pyroxenes, quartz, biotite and Fe-Ti oxides. Among 566 grains of hornblende phenocrysts observed, 503 grains are completely decomposed. We quantified degree of hornblende breakdown (DHB) by image analyses of BSE images for remaining 62 grains incompletely decomposed. DHB varies from 18 to 98 %.

Chemical analyses were done for incompletely decomposed hornblende grains by using EPMA (JEOL-8800R) at Earthquake Research Institute, University of Tokyo. Most of hornblende phenocrysts are chemically homogeneous. They are divided into two groups based on AlT [= number of Al per 23 oxygens] with ca. 1.2 and 2.1, respectively. negative correlation is observed between AlT and Si content and DHB increases with Si content. All of analyzed hornblende show Al# [=[6]Al/ AlT] lower than 0.21 and satisfy criterion for applying hornblende geothermobarometer of Ridorfi et al. (2010). Using the geothemobarometer, equilibrium pressure and temperature conditions are estimated for hornblende. The estimated pressures show two separated ranges of ca. 100-200 and ca. 350-450 MPa, corresponding to depths of ca. 2.5-5 and ca. 8.5-11km, respectively. Estimated temperatures are ca. 820-920 and ca. 970-1000 degree C for low-P and high-P hornblende phenocrysts, respectively. DHB tends to increase as estimated temperature decreases.

Present results indicate that there were at least two separated magma reservoirs at depths of 2.5-5 and ca. 8.5-11km. The depth of the deeper reservoir is consistent with that inferred from geothermal study of Furukawa (2009), implying the reservoir has existed at least since ca. 7-10 ka. On the other hand, depth range of the shallower reservoir is consistent with that of aseismic zone beneath Tsurumi volcano reported in Ohkura et al. (2002). The consistency may imply that the shallower reservoir contributed to form the aseismic zone.

Coexistence of hornblende phenocrysts with different P-T conditions is consistent with that the lava was formed by magma mixing as pointed out by Ohta et al. (1990, 1991). Mixing of high-T and low-T magmas derived from deeper and shallower reservoirs induced rapid decomposition of low-P hornblende due to heating, but decomposition of high-P hornblende was insignificant because of mixing-induced cooling. High-P hornblende was decomposed during eruption due to degassing. Absence of low-P hornblende with low DHB indicates that post-mixing crystallization was insignificant and eruption occurred right after magma mixing.

Keywords: hornblende, Tsurumi-dake, geothermobarometry, magma chamber

Japan Geoscience Union Meeting 2015
(May 24th - 28th at Makuhari, Chiba, Japan)

SVC46-P03 Room:Convention Hall Time:May 25 18:15-19:30

Zoning pattern analyses of plagioclase phenocrysts in Fuji-Jogan magma; constraints on pre-eruptive magma process

MIWA, Haruna[2] ; ISHIBASHI, Hidemi[1*]

[1]Guraduate School of Science, Shizuoka university, [2]Faculty of Science, Shizuoka University

Jogan eruption occurred at 864-866 at northwest flank in the largest historical eruption of Fuji Volcano. During the eruption, more than 1.3km3 of relatively homogeneous differentiated basaltic lava was effused. In addition, most of the lava was effused in the first two month of the eruption duration, indicating contribution of large magma reservoir. Our interest is in the pre-eruption processes in its magma reservoir.

Plagioclase composition sensitively depends on coexisting melt compositions, melt water content, temperature and pressure. In addition, compositional zonation is not significantly modified due to slow CaAl-NaSi diffusion in plagioclase. These characteristics allow us to decipher magma processes such as crystallization, magma mixing and eruption from compositional zonation of plagioclase phenocrysts. In this study, we focused on compositional zoning patterns of plagioclase phenocrysts in the Jogan basaltic rocks to decipher pre- eruption processes the magma experienced in its reservoir

In this study, plagioclase phenocrysts in two basaltic ejecta, Nagaoyama lava and Nagaoyama scoria, are investigated. BSE images were acquired for 187 and 87 plagioclase phenocrysts in Nagaoyama lava and Nagaoyama scoria, respectively, by using SEM at Michibayashi lab., Shizuoka University. We classified plagioclase phenocrysts into five groups based on gray scale intensity zoning patterns. In addition, chemical analyses were done for representative grains by using EPMA (JEOL 8800R) at Earthquake Research institute, University of Tokyo.

Comparison of BSE image and compositional map indicates that An content [=Ca/(Ca+Na]] is responsible for gray scale intensity in BSE images. Plagioclase phenocrysts in Jogan basalt are classified into the following five groups; (A) normally zoned grains with An-rich homogeneous core, (B) grains showing narrow, strong reverse zoning at boundary between An-poor core and normally zoned rim, (C) oscillatory zoned grains, (D) grains with irregular zoning pattern, and (E) homogeneous grains. Type D and E grains are rare and Type B grains are most abundant. We cannot find grain with reverse zoned rim. Core of type A grain shows An content higher than that observed in any part of type-B grain. Wavy boundary and alignment of melt inclusions are observed at core-rim boundary in type B plagioclase.

Monotonous crystal growth explains normal zonation shown in Type A phenocrysts. Magma mixing is required to explain zoning pattern in type B grains; An-poor homogeneous plagioclase was once melted by magma mixing and then overgrown with An-rich composition to form Type B phenocrysts. Textures observed at core-rim boundary is consistent with this interpretation. Repeated magma mixing and crystallization formed type-C grains. Presence of oscillatory zoned plagioclase indicates that magma replenishment, crystallization, crystal fractionation and eruption have been repeated in this magma reservoir. With considering high effusion rate of basaltic magma in the 864-866 eruption, the reservoir was one of main long-lived ones in Fuji Volcano. Normal zoned rim parts observed in most of plagioclase phenocrysts were interpreted to form during eruption because no discontinuity in zoning pattern is observed in this parts. In type B plagioclase, the rim part is neighboring with reverse zoned part formed by magma mixing, suggesting that eruption occurred right after magma mixing.

Keywords: Fuji volcano, plagioclase, Compositional zoning, magma chamber, Jogan eruption

Japan Geoscience Union Meeting 2015
(May 24th - 28th at Makuhari, Chiba, Japan)

SVC46-P04 Room:Convention Hall Time:May 25 18:15-19:30

Groundmass texture of B-fall deposit from the Ten-nin eruption, Asama volcano, Japan

HONGO, Yuko[1] ; NAKAMURA, Michihiko[1] ; OKUMURA, Satoshi[1*] ; MUJIN, Mayumi[1]

[1]Department of Earth Science, Graduate School of Science, Tohoku University

Volcanic eruptions often show the transition from explosive to non-explosive activities and the change in the explosivity during explosive activity. A controlling factor of the explosivity is the magma ascent velocity in volcanic conduits (e.g. Jaupart and Allegre, 1991). When the velocity of magma ascent is high, magma does not experience gas loss, which results in explosive activity. On the other hand, non-explosive eruption is caused if magma ascent velocity is low and efficient outgassing occurs. In this study, we investigated crystal size distribution (CSD) of plagioclase microlite because it reflects magma decompression rate. We measured the CSD in fallout pumices from the Ten-nin eruption of Asama volcano and compared the CSD with those of other eruptions. The fallout deposit of the Ten-nin eruption is divided into eight subunit layers from B-1 to B-8. Four layers (B-2, B-4, B-6 and B-8) are composed of gray and brown pumices, while other layers, i.e., B-1 and B-5, and B-3 and B-7, are formed by volcanic ash and dense lithic fragment, respectively. The B-4, B-6 and B-8 also contain dense lithic fragment. All the samples investigated in this study have a common bulk chemical composition (Hongo et al., Volcanological Society of Japan, 2013). We analyzed bulk density and CSD for the pumices from B-4, B-6 and B-8. To obtain the CSD, we corrected the effect of microlite shape using CSD Slice5 software (Morgan and Jerram, 2006) and CSD corrections software (Higgins, 2000) after measurement of the length and number of the microlites on backscattered electron images with 800 magnifications. The vesicularities and crystallinities of B-4 and B-6 were smaller than those of B-8. The CSD slope was slightly steeper than those of B-4 and B-6. We compared the CSD obtained in this study with those of explosive to non-explosive eruptions reported by previous studies. The CSD data show that the slopes of the explosive eruptions are generally steeper than those of the non-explosive ones. This result implies that the CSD slope reflects magma ascent velocity and eruption style, but we need more data to clarify the relationship between CSD and eruption style, since no clear difference was found in some CSDs of sub-Plinian and lava dome eruptions (e.g. Castro and Gardner, 2008).

Keywords: crystal size distribution, microlite, pumice, sub-Plinian eruption, Asama volcano

Japan Geoscience Union Meeting 2015
(May 24th - 28th at Makuhari, Chiba, Japan)

SVC46-P05 Room:Convention Hall Time:May 25 18:15-19:30

Development process and controlling factors of bubble waves in bubbly flow

KINOSHITA, Akane[1*] ; TORAMARU, Atsushi[2]

[1]Department of Earth and Planetary Sciences, Graduate School of Sciences, 33 Kyushu University, [2]Department of Earth and Planetary Sciences, Faculty of Sciences, 33 Kyushu University

The hydrodynamic behavior of a two-phase system is investigated by an analog experiment. Bubbly flows with spatially periodic distribution of bubbles are sometimes observed in various natural situations such as in the conduit and lava flow. For instance, the early stage of the 1986 fire fountain eruptions of the Izu-Oshima volcano had the continuous magma effusion with a rhythm of mean period about 5s. This suggests the inhomogeneous distribution of bubbles in the conduit. The similar structure of bubble distributions is observed in a glass of Guinness beer. The bubbles are distributed nearly uniformly at the moment Guinness beer is poured, and quickly form layers or waves which appear to propagate downward. Unfortunately, Guinness is not appropriate for scientific experiment because of difficulties to control parameters (e.g. volume fraction and radii of bubbles), formation and dissolution of bubbles, and poor reproducibility of initial conditions such as pouring condition. We therefore conducted an analog experiment using the special liquid and the hollow glass particles as analog materials of a beer liquid and bubbles, respectively, presuming that the bubble waves in Guinness form by the relative motion of bubbles to liquid by buoyancy, but not by the formation and dissolution processes. We mixed the liquid and the particles in cylindrical test tube by gently shaking the test tube. The bubble segregation or relative upward migration of bubbles starts from the homogeneous mixture as an initial state just after stopping shaking. We found that under some conditions, the bubble waves form during the upward segregation of bubbles. In order to constrain factors for the formation of bubble waves, we conducted the series of experiments with varying the volume fractions, sizes of bubbles and the inclination of a test tube. We found that the bubble waves formed only when we incline the test tube, and when volume fractions of the particles are less than approximately 30 %. If we settled the test tubes vertically, the bubble waves didn't form. On the other hand, when we inclined the test tubes, we observed that the circulatory current of the particles directed upwards near the inter surface at higher wall of the test tube and downwards near the lower wall of it. The wave like structure of the particles with the wave length about 10-20 mm and the horizontal width about ˜5mm developed near the lower wall of the inclined test tube. The wave length and the horizontal width of bubble waves were inversely proportional to the inclined angle of the test tube and the volume fraction of the particles. We propose the formation mechanism of bubble waves on the basis of the Kelvin-Helmholtz instability which develops at the thin boundary layer formed near the lower wall, where the downward bubble-poor and overlaid upward bubble-rich layers contact each other.

Keywords: bubbly flow, inhomogeneous distribution of bubbles, analog experiment

Japan Geoscience Union Meeting 2015
(May 24th - 28th at Makuhari, Chiba, Japan)

SVC46-P06 Room:Convention Hall Time:May 25 18:15-19:30

Direct molecular dynamics simulations of homogeneous bubble nucleation and improvements of classical theory

TANAKA, Kyoko[1*] ; TANAKA, Hidekazu[1] ; DIEMAND, Juerg[2] ; ANGELIL, Raymond[2]

[1]Institute of Low Temperature Science, Hokkaido University, [2]University of Zurich

Bubble nucleation in liquid is a liquid-to-vapor transition phenomenon and plays an important role in vulcanism. Studies of homogeneous liquid-vapour nucleation typically use the classical formula (CNT) for the bubble nucleation rate. However, the applicability of the CNT is not well understood.

Numerical techniques such as molecular dynamics and Monte-Carlo simulations are powerful methods to resolve details of the nucleation process and provide useful test cases for nucleation models. Typically, these simulations show large deviations from the CNT predictions. Most of the simulations for bubble nucleation in the literature use around 10^5 or fewer atoms, making it difficult to measure nucleation rates directly.

Recently, we presented large-scale, micro-canonical molecular dynamics simulations of homogeneous bubble nucleation with $5 * 10^8$ Lennard-Jones atoms, and succeeded to directly measure nucleation rates in the range of $10^{21-25}\mathrm{cm}^{-3}\mathrm{s}^{-1}$ for argon by resolving bubble nucleation events in the steady state nucleation phase [1,2]. The unprecedented size of the simulated volumes allows us to resolve the nucleation and growth of many bubbles per run in simple direct micro-canonical (NVE) simulations while the ambient pressure and temperature remain almost perfectly constant.

We find bubble nucleation rates which are lower than in most of the previous, smaller simulations. It is widely believed that classical nucleation theory (CNT) generally underestimates bubble nucleation rates by very large factors. However, our measured rates are within two orders of magnitude of CNT predictions - only at very low temperatures the CNT underestimates the nucleation rate significantly.

We also derive an improved classical formula for the homogeneous bubble nucleation rate, where we revise the prefactor in the nucleation rate and compare it with the widely used classical nucleation theory (CNT) [3]. Our large-scale molecular dynamics simulations and laboratory experiments for argon bubble nucleation enable us to precisely test our theoretical models. The improved formula including the Tolman correction with a small positive Tolman length leads to good agreement with both MD simulations and laboratory experiments.

[1] J. Diemand, R. Angelil, K. K. Tanaka, and H. Tanaka, Pys. Rev E 90, 052407 (2014)
[2] R. Angelil, J. Diemand, K. K. Tanaka, and H. Tanaka, Pys. Rev E 90, 063301 (2014)
[3] K. K. Tanaka, H. Tanaka, R. Angelil, and J. Diemand, submitted

Keywords: bubble nucleation, liquid to vapor transition, phase transition, molecular dynamics simulation

Japan Geoscience Union Meeting 2015
(May 24th - 28th at Makuhari, Chiba, Japan)

SVC46-P07 Room:Convention Hall Time:May 25 18:15-19:30

Numerical analysis of the behavior of a viscoelastic body containing gas bubbles by rapid decompression

KUROKAWA, Noriaki[1*] ; KAMEDA, Masaharu[1] ; ICHIHARA, Mie[2]

[1]Mech. Sys. Eng., TUAT, [2]ERI, Univ. of Tokyo

Brittle fragmentation of vesicular magma is considered to be a trigger of explosive volcanic eruptions. Ichihara and Rubin (2010) defined the brittleness as a dominant parameter of the brittle fragmentation of magma. They concluded that the brittle fragmentation occurred when the brittleness of magma was close to unity. Kameda et al. (2013) reported that the brittle-like fragmentation occurred in their laboratory experiments even if the brittleness of specimen was lower than unity. They suggested that the brittle-like fragmentation was initiated by the crack developed from the interior of the specimen due to non-uniform spatial distribution of bubbles. After the partial fragmentation occurs, the rapid decompression around the fracture surface induces sequential fragmentation events.

In this study, to verify the scenario of the brittle-fragmentation proposed by Kameda et al., we simulated numerically the behavior of a Maxwell viscoelastic body including a few bubbles due to rapid decompression. We examined the evolution of the differential stress and brittleness around the bubbles in viscoelastic body.

We used COMSOL multiphysics ver. 5.0 as the platform for our numerical analysis. We employed axial symmetry model as the space dimension, and generalized Maxwell viscoelastic model as the viscoelastic model. In the first case (Case 1) of our calculation, we set the calculation area as a hemisphere (a quarter of a circle which radius was 100 mm), and arranged two spherical bubbles in the area. The large bubble (radius is 20mm) was located at the central point of the hemisphere. Another small bubble (radius is 5 mm) was located at the isolate position beneath the large bubble, and its central point was placed on the symmetry axis of the hemisphere. The physical property of the viscoelastic body and the profile of decompression were the same values as the laboratory experiment. We assumed the internal pressure of bubbles remained a constant value.

In Case 1, the stress concentration is observed at the surface of small bubble facing the large bubble. In contrast, smaller differential stress is observed at the surface of large bubble facing the small bubble. To investigate this reason, we calculated the numerical analyses (Case 2, 3) using the geometry of Case 1. In Case 2, internal pressure was applied only on the large bubble. In Case 3, the internal pressure was applied only on the small bubble. These results showed stress concentration is observed at the surface of small bubble only in Case 2.

We propose the following scenario of stress concentration: There is the influence range on the distribution of differential stress around the bubble. The range spreads as the size of bubble becomes large. If the bubble exists in the influence range of differential stress produced by the other bubble, stress concentration occurs on the surface of bubble.

In Case 4, we calculated the time variation of the brittleness with considering the change of the internal pressure of the bubble due to its expansion. We calculated the stress field around a single bubble placed spherically symmetric position in the domain. The volume of the bubble is equal to the sum of the volume of the bubbles in Case 1. We assumed that the internal pressure of the bubble varied isothermally. The results showed the time variation of the brittleness on the bubble's surface in Case 4 was not so different from Case 1. On the other hand, the maximum value of the differential stress around the bubble was developed steeper in Case 1 than in Case 4. This means that the critical brittleness, which is defined as the brittleness at the time when the maximum differential stress reaches the critical fracture stress, is higher in Case 1 than in Case 4.

In conclusion, (1) Stress concentration occurs at the bubble's surface in the case where neighboring bubbles are close to their bubble radii. (2) The critical brittleness at the position where stress concentration occurs becomes large.

Keywords: Magma, Viscoelasticity, Fragmentation, Numerical analysis

Japan Geoscience Union Meeting 2015
(May 24th - 28th at Makuhari, Chiba, Japan)

SVC46-P08 Room:Convention Hall Time:May 25 18:15-19:30

X-ray CT observation of fragmentation of vesicular magma analogue

AOKI, Yamato[1*] ; KAMEDA, Masaharu[1] ; TSUGO, Mitsuaki[1] ; YAMADA, Akihumi[1] ; ICHIHARA, Mie[2] ; OKUMURA, Satoshi[3] ; UESUGI, Kentaro[4]

[1]Mech. Systems Eng.,TUAT, [2]ERI, Univ. of Tokyo, [3]Earth Sci., Tohoku Univ., [4]JASRI

”Explosive eruption” of volcano adversely affects to our lives. The explosive eruption may be triggered by the rapid discharge of gas in vesicular magma due to its brittle fragmentation. We focused our attention to the ”brittle-like fragmentation” (Kameda et al. JVGR 2013) which was defined as the solid-like fracture of the material whose bulk rheological properties was close to fluid state. We tackle to elucidate the mechanism of the brittle-like fragmentation by laboratory experiment.

Recent our laboratory experiment (Shida et al. IAVCEI 2013) showed that the onset of brittle-like fragmentation depended on the size of specimen even if the bulk rheological properties and void fraction remained constant. The probability of the fragmentation decreases as the size decreases. In our experiments, the heterogeneity of spatial and size distribution of the bubbles was more remarkable in larger specimen than in smaller one. We guess that this heterogeneous distribution of the bubble in the specimen is a main source of the brittle-like fracture.

On observing the behavior of the fracture, we use the syrup as magma analogue. The syrup is suitable for the magma analogue because its rigidity is close to the rigidity of magma, and its viscosity is varied widely by hydration or dehydration. Furthermore, we add H_2O_2 and MnO_2 into the syrup and generate O_2 gas bubbles to mimic the vesicular magma. We use the rapid decompression equipment to observe the fracture of the specimen. It consists of the pressure container whose top is sealed by plastic (Lumirror) film. A thin nichrome wire is bonded to the film. We set the specimen in the pressure container, and pressurize the container by filling nitrogen gas up to our desired value. After pressurization is completed, we energize the nichrome wire by rapid current discharge from capacitor. The film is abruptly ruptured by the heat of the nichrome wire, then rapid decompression attacks the specimen. The specimen has a hemispherical shape whose diameter is about 20mm. We choose the viscosity of each specimen in the range from 10 MPa s to 200 MPa s. The initial pressure before decompression is 2 MPa. The characteristic time of decompression (the time when the pressure in the container reach 1/e of the initial value) is about 5 - 7 ms.

We conducted the X-ray micro CT imaging at BL20B2 in SPring-8 (JASRI) to observe the internal structure of the specimen. We took the transmission images of the specimen whose viewing angle was varied from 0 to 180 degrees every 0.1 degree. Each captured image has 2048 pixels in width and 1400 pixels in height. We conducted the CT imaging before compression, after compression, and after rapid decompression (at atmospheric pressure). We also captured the dynamic behavior of the specimen during decompression by high-speed radiography (100 fps).

From these experiments, we found that the fracture occurred at the parts where the large bubbles were accumulated. In contrast, the fracture did not occur at the parts where a large bubble independently existed. Furthermore, we found that the fracture may occur when the inter-distance of neighboring bubbles is close to the order of the bubble radius, even if the rheological bulk properties of the specimen is close to the fluid state (the brittleness is not near unity).

Keywords: Magma, Fragmentation, Rapid decompression, Brittleness, X-ray CT, Non-uniform distribution of bubbles

Japan Geoscience Union Meeting 2015
(May 24th - 28th at Makuhari, Chiba, Japan)

SVC46-P09 Room:Convention Hall Time:May 25 18:15-19:30

Estimating of the maximum volume of magma accumulation in the crust before a large volcanic eruption

FUJITA, Shiori[1*] ; SHIMIZU, Hiroshi[2]

[1]Department of Earth and Planetary Sciences, Graduate School of Sciences, Kyushu University, [2]Institute of Seismology and Volcanology, Faculty of Sciences, Kyushu University

Massive volcanic eruption, which emits several hundred cubic kilometres of magma and often forms huge calderas afterwards, occurs around once in every 10000 years in Japan. Although it is necessary for a huge amount of magma to accumulate in the crust for such a big eruption, there has been little quantitative analysis to determine the critical value of mechanical magma accumulation in relation to the depth and shape of the magma chamber and magma accumulation rate.

While the long-term magma accumulation rate at the volcano was estimated to be about 0.001-0.01km^3/yr inferred from the magma volume of past eruption, Druitt et al. (2012) suggest the possibility that a massive store of about 10km^3 magma had accumulated for around just 100 years before the eruption, based on an analysis of Mg concentration in plagioclase crystals of Santorini pumices. This result indicates an extraordinarily large magma accumulation rate of 0.05-0.1km^3/yr, and recently such a huge rate has actually been observed in some volcanoes. For instance, Chang et al.(2010) obtained a magma accumulation rate of 0.06-0.07km^3/yr in 2005-2008 from GPS and InSAR survey at Yellowstone caldera. InSAR observation also indicated a magma accumulation rate of 0.03km^3/yr at Uturuncu volcano in Bolivia (Sparks et al.2008). These research results show that in some cases magma is able to move abruptly upward and accumulate for a term of at least 100 years. Because the stress relaxation time of the crust as viscoelastic body is much longer than this time scale, the response of the crust to such a speedy magma accumulation can be treated as elastic deformation.

In this study, we posit the volume of magma accumulation in the crust which is possible over a time period shorter than the stress relaxation time of the crust. We calculate crustal deformation, strain and stress based on several magma chamber's depth, shape and volume pattern, and compare these with the limit strain of the crust. We presumed the shape of the magma chamber to be a sphere, dyke, or sill with a depth of several to a dozen kilometers. We used the crustal deformation calculation model for an elastic body proposed by Okada (1992).

We assumed a spherical magma chamber 10km deep and a volume change of 10km^3 when the magma accumulation rate is huge, and therefore the crust is regarded as a perfect elastic body. In this case, the strain value exceeded the crustal limit strain of 10^{-4} within a 30 km radius. This result indicates the crust around magma chamber yields and plastic deform before 10km^3 accumulation or causes brittle fracture as to a spherical magma chamber 10km deep.

Keywords: large volcanic eruption, magma accumulation, crust, strain, stress, caldera

Japan Geoscience Union Meeting 2015
(May 24th - 28th at Makuhari, Chiba, Japan)

SVC46-P10 Room:Convention Hall Time:May 25 18:15-19:30

Parameterization of conduit flow model based on the inverse analysis of data from ground deformation and magma extrusion

MATSUO, Naoya[1*] ; KOYAGUCHI, Takehiro[1] ; SUZUKI, Yujiro[1]

[1]Eartuquake Research Institute, The University of Tokyo

During volcanic eruptions, slight changes in geological conditions often result in various types of eruptions such as effusive and explosive eruptions. In order to understand such complexities of conduit flow dynamics, several conduit flow models have been proposed (e.g., Melnik and Sparks, 2005). In the conduit flow models, temporal evolution of pressure and velocity in the conduit are calculated from model parameters such as volume of magma chamber and magma properties. In order to forecast the transitions of eruptions, these model parameters need to be estimated from the inverse analysis of time-series data of observation. Anderson and Segall (2013) formulated a posterior probability density function of model parameters given ground deformation and magma extrusion data based on Bayes' theorem, and yielded probabilistic estimates for the model parameters using a Markov Chain Monte Carlo (MCMC) algorithm. However, because their inverse analysis includes many model parameters, it is difficult to understand the influence of each observation on the parameter estimation. The present study aims to systematically investigate the influence of ground deformation and magma extrusion data on parameter estimation, and ultimately, to estimate model parameters of a more sophisticated conduit flow model that takes into account the effects of gas escape and crystal growth during magma ascent (e.g., Kozono and Koyaguchi, 2012).

In this study, a model consists of the magma plumbing system where pressure of a spherical magma chamber in elastic rocks is determined by the balance between magma influx and outflux. We also assume that conduit flow is determined by the balance between pressure gradient and viscous force (i.e., Poiseuille flow). In this system, model parameters include chamber volume, conduit length, effective elastic modulus of magma in the chamber and the chamber itself, conduit radius, magma density and viscosity. On the other hand, observables include the time-series data of the volume change due to inflation/deflation of the chamber (ΔV_G) and the amount of extruded magma (ΔV_E).

Assuming that magma density and viscosity are constant in the conduit, extrusion rate Q and magma chamber pressure P approach the steady solution (Q_s,P_s) with a time constant τ. A parameter τ is determined by chamber volume, effective elastic modulus, magma viscosity, conduit radius and conduit length. In the case where τ can be estimated from the time-series data of ΔV_G and ΔV_E, the estimated value of τ provides the information related to the conductivity of the conduit flow and the system size, whereas the difference between ΔV_G and ΔV_E provides the information related to magma compressibility and the shape of the chamber.

We have also preliminarily investigated the influence of gas escape and crystal growth on the parameter estimation assuming various function forms for magma density and magma viscosity. In this preliminary study, we compare the probability density distribution of model parameter estimated numerically using a MCMC algorithm with the analytical results in order to understand how the parameter estimation using MCMC algorithm is applicable to the problems of complex conduit flows with gas escape and crystal growth.

Keywords: volcanic eruption, conduit flow, lava dome, ground deformation, inverse analysis

Japan Geoscience Union Meeting 2015
(May 24th - 28th at Makuhari, Chiba, Japan)

SVC46-P11 Room:Convention Hall Time:May 25 18:15-19:30

Sawtooth wave-like pressure change and cyclic out-gassing observed in laboratory experiments

KANNO, Yo[1*] ; ICHIHARA, Mie[1]

[1]The Earthquake Research Institute, the University of Tokyo

1.Introduction

A sawtooth wave-like (SWT) pressure change was observed in laboratory syrup eruption experiments (Kanno and Ichihara, 2014,VSJ fall meeting).

Sawtooth wave-like infration-defration cycles have been observed with eruptions at many volcanoes (Genco and Ripepe 2010, Lyons et al. 2012, Nishimura et al 2013). We expect that clarifying the mechanism of a similar oscillation in this experiments helps understanding the actual volcanic phenomena. Conduit flow patterns are controlled by the gas volume fraction and relative velocity between liquid and gas (Vergniolle and Jaupart, 1986). Supposing that the SWT pressure oscillation was generated by transitions of flow patterns, we conducted experiments on flow in a tube with varying fluid rheology and injected gas flux. However we never observed the SWT oscillation.

In this study, we examine effects of the chamber below the tube on generation of the SWT oscillation.

2.Equipment and Method

Gas is injected to a transparent tube to generate alternate layered flow of syrup and gas. The viscosity of the syrup is about 1 Pa.s. The diameter of the tube is 5 mm. An acrylic chamber (ϕ=50 mm, H=100 mm) is attached beneath the tube. A pressure transducers is mounted at the injection point in the tube and another at the bottom of the chamber. In addition, a microphone is mounted at the exit of the tube. Flow in the tube is recorded with a high-speed camera (Fig.1a).

We inject the syrup in the tube to the height of 60 mm from the bottom of the tube. In order to keep the syrup within the tube, we use a 800-mm long tube. We partially fill the chamber with water and control the volume of the chamber (Vc) by changing the amount of water. Injected gas flux (Qin) is controlled by a regulator.

3.Result

We control Vc from 0 to 120 cm^3 and Qin from 0.1 to 30 μ m^3/s for each Vc.

(1) Changing Vc with constant Qin

For small values of Vc, quasi-sinusoidal pressure oscillation is observed with periodic ruptures of syrup layers at the top. The velocity and the thickness of the following syrup layers are nearly constant with a minor influence of the rupture.

The SWT oscillation is observed for sufficiently large Vc (Fig.1b). In this case, all syrup layers burst simultaneously to make pressure drop. After this event, syrup layers recover with deformation of syrup film flowing down the inner wall, and the pressure in the chamber starts to increase gradually. The syrup layers are accelerated with the pressure increase and their thicknesses become thinner. Then, the syrup layers burst again to cause pressure drop.

(2)Changing Qin with constant Vc

When Vc is small, quasi-sinusoidal pressure oscillation is observed in all the experimental range of Qin. The period of the oscillation is smaller when Qin is larger. When Vc is sufficiently large, the SWT oscillation appears intermittently among the quasi-sinusoidal oscillation. The SWT oscillation dominates when Qin further increases.

4.Discussion

For volcanic systems, asymmetric pressure change has been explained by a coupling mechanism among pressure in a magma chamber, conduit flux, and viscosity (Ida,1996; Barmin et al,2002; Nakanishi and Koyaguchi,2008).

Based on these models, we considered two effects:

(1) Viscous dissipation in the tube becomes larger (smaller) when the thicknesses of the syrup layers increase (decrease).

(2) The chamber plays a role of a buffer.

With these assumptions, the experimental system is formulated by simple ordinary differential equations.

This model generates a SWT pressure change with increasing Vc at constant Qin (Fig.1c). When Vc is small, quasi-sinusoidal pressure oscillation is generated. For constant Vc, the waveform gradually changes from SWT to quasi-sinusoid with decreasing Qin.

In this way, the model can qualitatively simulate the oscillation patterns that are observed in the laboratory experiments. In the

future, we will study effects of each parameter in more detail.

Keywords: Sawtooth wave, Analog experiment, Multi phase flow, Magma chamber, Conduit flow, Tilt motion

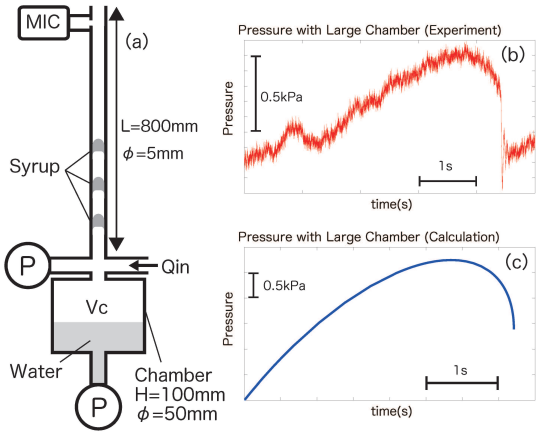

Japan Geoscience Union Meeting 2015
(May 24th - 28th at Makuhari, Chiba, Japan)

SVC46-P12 Room:Convention Hall Time:May 25 18:15-19:30

Variation of VLP signals accompanying eruptions at Stromboli volcano, Italy

YAMADA, Taishi[1*] ; AOYAMA, Hiroshi[1] ; NISHIMURA, Takeshi[2] ; KAWAGUCHI, Ryohei[3] ; MIWA, Takahiro[3] ; FUJITA, Eisuke[3] ; RIPEPE, Maurizio[4] ; GENCO, Riccard[4] ; LACANNA, Giorgio[4]

[1]Faculty of Science, Hokkaido University, [2]Graduate School of Science, Tohoku University, [3]National research Instituite for Earth science and Disaster prevention, [4]Dipartimento Scienze della Terra, Universita di Firenze

Stromboli volcano in Italy, one of the most active and famous volcano in the world, has been the target field of volcanology to understand eruption dynamics. From aspect of volcano seismology, broadband seismic observations have revealed that VLP(very-long-period) signals (10˜sec) are dominant among the seismic signals accompanying eruptions at Stromboli volcano (e.g. Neuberg et al., 1994). Chouet et al. (2003) demonstrated that inflation-deflation-inflation sequence of moment components, which represent inclined crack, is dominant at VLP signals observed at Stromboli volcano. The estimated force system was considered to represent the rise and ejection of gas slug, which causes repressurization of crack corresponding second inflation. However, most previous researches have analyzed a few VLP events having specific waveform characteristics, that were typical among their temporary observation data for days or weeks.

We have conducted broadband seismic observation at Stromboli volcano since May 2014. From 4 month long broadband seismic record, most VLP events seem to have similar waveform characteristics mentioned in Chouet et al. (2003) (inflation-deflation-inflation sequence). However, we recognized there are several waveform types prior to main first inflation phase.

1. Gradual inflation (10 ˜30 sec) prior to main inflation
2. Having small deflation phase (˜5 sec) during gradual inflation (type 1)
3. Gradual deflation (10 ˜30 sec) prior to main inflation
4. Combination of type 2 and 3
5. Short deflation (˜5 sec) prior to main inflation
6. No main inflation phase (Only downward pulse)

As described above, there are certain groups of VLP events which have deflation phase prior to main first inflation phase. Even if amplitude of deflation phase is small, such deflation process cannot be explained by the simple gas slug rising model. Moreover, some VLP events (type 6) have no inflation phase at the onset. Particle motion analysis for onset and first inflation phase shows events in type 1, 2, 5, 6 have common azimuthal direction (NW-SE direction), while events in type 3, 4 have slightly different direction. Since Stromboli volcano has several active vents on the northwest direction from our seismic station, these differences of azimuthal motions may reflect the difference of vents where eruptions were taken place. Another remarkable feature is about the transition of occurrence frequency of each type. For example, occurrence frequency of type 6 has decreased at the beginning of Aug. 2014. Those days correspond to the period that amplitude of RMS (root-mean-square) of high frequency ($>$3 Hz) has decreased. Also transition of eruption style has been reported at that period, from intermittent Strombolian eruptions to lava outflow and effusive eruptions.

Keywords: Strombolian eruptions, VLP, explosion earthquakes

Japan Geoscience Union Meeting 2015
(May 24th - 28th at Makuhari, Chiba, Japan)

SVC46-P13 Room:Convention Hall Time:May 25 18:15-19:30

Relative hypocenter determination of eruption earthquakes using deconvolution: Application to Stromboli volcano

SUGIMURA, Shunsuke[1*] ; NISHIMURA, Takeshi[1] ; AOYAMA, Hiroshi[2] ; YAMADA, Taishi[2] ; FUJITA, Eisuke[3] ; KAWAGUCHI, Ryohei[3] ; MIWA, Takahiro[3]

[1]Graduate School of Science, Tohoku University, [2]Faculty of Science, Hokkaido University, [3]NIED

Eruption earthquakes are repeatedly observed with intervals of several minutes, hours or days associated with Strombolian or Vulcanian explosions. These eruption earthquakes generally have obscure onsets of P or S phases, which disables us to use general hypocenter determination methods using the arrival times of these waves. In this study, we determine relative hypocenter locations of eruption earthquakes associated with repetitive eruption, using deconvolution filter and master event method.

We use records of three tilt meters that are deployed near the active crater of Stromboli volcano since May 2014. We analyze tilt signals of eruption earthquakes that are recorded with a sampling frequency of 100Hz. We relate arrival time difference between a master event and slave event at each station with differences of hypocenter parameters. We use deconvolution filter to obtain arrival time difference because eruption earthquakes observed at each station have similar waveforms. However, since the origin time of the master event is not known, we further calculate time differences of the arrival time differences between two stations to eliminate the origin time difference.

We analyze 31 eruption earthquakes occuring from 0:00 a.m. to 3:00 a.m., July 1of 2014, whose amplitudes are more than 20 micro radian at all the stations. We define the first event as a master event. Assuming the epicenter at NE crater, the depth of 100m for master event, and the wave velocity of 800m/s, we determine relative depths of slave events using least squares methods. The results show that the relative depths are estimated to be from 70 to 225m.

Deconvolution filter enables us to automatically read the time differences of arrival time differences between two stations. By analyzing large number of data, we will be able to monitor the spatio-temporal change of the source locations of repetitive eruptions.

Keywords: hypocenter determination, eruption earthquake, master event method, deconvolution, Stromboli volcano

Japan Geoscience Union Meeting 2015
(May 24th - 28th at Makuhari, Chiba, Japan)

SVC46-P14 Room:Convention Hall Time:May 25 18:15-19:30

NW-SE trending graben structure and crater row on Teishi Knoll, off Izu Peninsula

MINAMI, Hiroki[1*] ; IWABUTI, Yo[1]

[1]Hydrographic and Oceanographic Department, Japan Coast Guard

Teishi knoll, located 4 km off eastern Izu Peninsula, is submarine volcano of the Higashi-Izu monogenetic volcano group. Hydrographic and Oceanographic Department of Japan Coast Guard (JHOD) monitors and surveys the maritime and submarine volcanoes in Japan and we conducted bathymetric survey of Teishi knoll with survey vessel and autonomous underwater vehicle (AUV). Though intensive bathymetric surveys were done after the 1989 eruption by JHOD (Oshima et al., 1991), the resolution of used echo sounder was lower than the latest one and the detailed morphology was not mapped. Our survey revealed that NW-SE trending graben structure formed on the Teishi knoll. In addition, four small craters were aligned with same NW-SE trending as graben. These surface deformations such as graben and crater row indicate behavior of magma in the subsurface.

1. Method

The survey was conducted in December 2014. Multibeam echo sounder EM302 installed on S/V Kaiyo and interferometric sonar GeoSwath Plus on AUV GondouS were used.

2. Result

The graben formed just southeast of the main crater. The length is 120 m, width 70 m and 1.5 m deep. The four small craters formed inside the main crater associated with 1989 eruption. The craters are aligned in the NW-SE direction and each crater has 20?50 m in diameter. NW-SE trending linear topographic high also formed between the graben and craters.

3. Interpretation

Yamamoto et al 1991 concluded that magma intrusion into the sediment blanket caused the eruption, vapor explosion. Okada and Yamamoto 1991 concluded that the tensile fault, N125E strike (?NW-SE) caused the magma intrusion to sedimentary layers. The relationship between magma intrusion and surface deformation and the depth of the top of the dike is approximately equal to half the width of graben (Mastin and Pollard 1988; Chadwick and Embley 1998). The relationship was applied to our result in the Teishi knoll. The graben width 70 m implies that the top of the dike beneath the graben was at about 35 m depth. There are no direct evidences that the graben formed associated with 1989 eruption. Considering that the crater row is aligning in same NW-SE direction, same width 70 m and lying on the same line as graben, the graben might be formed in the identical environment, that is 1989 eruption with dike intrusion.

Keywords: Higashi-Izu monogenetic volcano group, bathymetry, multibeam echo sounder, graben, crater row, dike

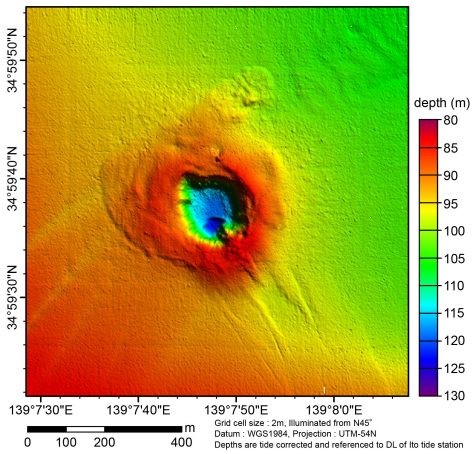

Japan Geoscience Union Meeting 2015
(May 24th - 28th at Makuhari, Chiba, Japan)

SVC46-P15 Room:Convention Hall Time:May 25 18:15-19:30

Variety of morphologies which are formed by molten lava-water interaction

NOGUCHI, Rina[1*] ; KURITA, Kei[1]

[1]Earthquake Research Institute, the University of Tokyo

There exists 2 types of responses when molten lava interacts with water environment: explosive and non-explosive. However, during eruption, it is difficult to make a judgment on whether explosion occurs or not. For example, in Nornahraun, Iceland, lava flowed into a river, but no explosion occurs to this day. This is a same as Nishinoshima Island. However, previous studies presented explosions which relate with lava-water interaction occurred in many places including Japan in the past [e.g. Mattox and Mangan, 1997; Ito and Taniguchi, 1996]. Its disaster risk has not been recognized; its explosivity would reach the degree of maar (magma-water interaction), and it is possible to generates low-concentration pyroclastic density current [Fagents and Thordarson, 2007]. Thus, it is important to understand this explosion mechanism for us Japan because of not only interesting of volcanic explosion but also prevention and reduction of disaster when lava flow into water environments near distinct of residence.

Today, it is known that there exists 3 types of morphometry which relates to lava-water interaction: rootless cones, spiracles, and lava pillars.

Lava-water explosive interaction have been well-known in basaltic volcanism, but previous studies showed it occurred in andesitic and rhyolitic [e.g. Hayakawa and Yui, 1989; Ito and Taniguchi, 1996]. Although their related-morphology has been studied, there remains problems to understand this phenomenon. Rootless cone (aka secondary crater and pseudocrater) is a typical morphology which is formed by lava-water interaction. They have a variety of shape; Hamilton et al., 2010 showed 3 archetypes of them which relates to flowing types of lava (tube-, channel-, and broad sheet lobe-fed). However, the relationship between their morphometry and formation conditions (e.g. explosivity, water/magma mass ratio, underlying sediments) has not been revealed. This is a problem for not only rootless cones but also other pyroclastic cones (e.g. scoria cone, maar, tuff cone). Rootless cones would be useful also in planetary science. Recent studies have found candidates of rootless cone on Mars [e.g. Greeley and Fagents, 2001]. These morphologies are expected to reveal recent 100Ma Martian magmatism. Thus this study could give great influence for planetary science. It is necessary to understand the variety of morphology and distribution of rootless cones to know the style of magmatism and environment.

Spiracles are found in bottom of lava flows as irregular shaped-vesicles which are formed by lava-water explosion. In Japan, cylindrical vesicles in Aokigahara lava flow was considered as typical spiracles for many years. Now its are considered as tree molds which were vertically-elongated by inflation of lava, and we lost an image of spiracle. Therefore we should reconstruct the image once again.

Lava pillars are considered as results of non-explosive lava-water interaction [e.g. Gregg et al., 2002]. They show chimney-like morphology, and has been found both in subaerial and submarine volcanism. Recently, Gregg et al., 2002; Gregg and Chirstle, 2013 showed that lava pillars were formed by water vaporization or hydrothermal activity at gaps of pahoehoe lava lobes. However, there exists lava pillars which were formed by a'a lava flow. Hence it remains problems for the lava pillar formation and non-explosive lava-water interaction.

In this presentation, we will review previous studies about morphologies which relate with lava-water interaction, and marshal problems to 1) understand volcanic explosion, 2) know its disaster risks, and 3) apply to planetary science. Especially focusing on rootless cone, we will discuss its variety of shapes based on our aerial photo analysis and field survey. Additionally, a new type of lava-water interaction-related morphology which we found both in Iceland (called as hraunbollar) and Hawaii will be introduced.

Keywords: lava-water interaction, explosion, rootless cone, spiracle, lava pillar

Japan Geoscience Union Meeting 2015
(May 24th - 28th at Makuhari, Chiba, Japan)

SVC46-P16 Room:Convention Hall Time:May 25 18:15-19:30

The influence of the linear increase in the source height on the 1D quasi-steady state fall and sedimentation processes

IRIYAMA, Yu[1*] ; TORAMARU, Atsushi[2]

[1]Department of Earth and Planetary Sciences, Graduate School of Sciences, Kyushu University, [2]Department of Earth and Planetary Sciences, Faculty of Sciences, Kyushu University

The stratigraphic variation of grain-size distribution (GSD) of pyroclastic fall deposit records the time variation which may reflect the time variation of GSD in the umbrella eruption cloud. In order to relate the stratigraphic variation of GSD and the time variation of umbrella eruption cloud GSD, it is necessary to consider the transportation process of ejecta.

Iriyama and Toramaru (2014, AGU) formulate the mathematical relationship between the depositional structure and the source (the umbrella eruption cloud upward in a vertical direction from the sedimentation point) parameters under the 1D constant height model in which the source height and the source GSD are constant with time throughout a release duration. In this case, we showed that the thickness ratio of the upper and lower layers, which is defined as the ratio of the thickness of the upper layer above the extinction point of the largest grain to whole layers depends on the ratio of the source height, the source GSD, and release duration. In nature, however, the eruption column height or ash cloud height may change even during continuous eruptions such as plinian type. In this study, we numerically assess the influence of the linear increase in the source height on the sorting structure of deposits in the simplest case.

When the linear increase rate in the source height is given as constant b, the increase in b makes the sedimentation duration longer than in the constant height model at the sedimentation surface. The numerical simulations for the linear increase height model are carried out with varying b under the same conditions of the initial source height, the source GSD, and release duration. Results show that the linear increase constant b have a negative correlation with the peak accumulation rate and have a positive correlation with the thickness ratio of the upper layer. These suggest that the increase in the source height (eruption intensity) can be detected from the thickness ratio of the upper layer which can be observed by the geological survey.

Keywords: pyroclastic fall deposits, grain-size distribution, development of eruption

Japan Geoscience Union Meeting 2015
(May 24th - 28th at Makuhari, Chiba, Japan)

SVC46-P17 Room:Convention Hall Time:May 25 18:15-19:30

The Tephra Fall Simulations of the Ignimbrite Eruption of Aso Volcano

ISHII, Kensuke[1*] ; SUZUKI, Yujiro[2] ; SHIMBORI, Toshiki[1] ; FUKUI, Keiichi[1] ; SATO, Eiichi[1]

[1]Meteorological Research Institute, [2]Earthquake Research Institute, The University of Tokyo

For aviation safety, Tokyo Volcanic Ash Advisory Center (Tokyo VAAC) of Japan Meteorological Agency (JMA) operates the tephra prediction system using the Global Atmospheric Transport Model (JMA-GATM) in which JMA Global Forecast or JMA Global Analysis (JMA, 2013) is applied to the atmospheric conditions. JMA-GATM calculates the time evolution of tephra dispersal due to the advection by wind, the diffusion, the gravitational settling, and the wet/dry deposition. Using this model, we have performed the tephra fall simulations for possible ignimbrite eruption (Tatsumi et al, 2014) at Aso volcano in Japan.

The ignimbrite eruptions had been occurred 4 times at the Aso volcano in the past 300,000 years. The Aso-4 ignimbrite eruption (90ka) is considered to be largest among these four eruptions. The tephra particles from this eruption were distributed widely in Japan (Aso-4 tephra); the tephra fall deposits in Hokkaido (1700km far from the volcano) have thickness of about 15cm. In this study, we performed the numerical simulations of tephra fall for the ignimbrite eruption whose intensity is comparable with the Aso-4. In these simulations, it is assumed that the constant emission of the tephra continues for 20 hours, and the total amount of tephra is $7.2*10^{14}$kg.

In JMA operation, an initial distribution of tephra particles for JMA-GATM is given from the estimation using the eruption column model (Suzuki, 1983) or the satellite observation. In the present study, we carried out a numerical simulation of eruption cloud using three-dimensional fluid-dynamics model (Suzuki et al, 2005) in order to estimate an accurate initial distribution of tephra particles. The tracer distribution at 3.5 hours from the initiation of eruption which are obtained from the 3D simulation is used as an initial setting for JMA-GATM. Because JMA-GATM calculates the time evolution of the tephra particles which are advected by wind, the particles with a large velocity difference from the wind are eliminated from initial setting. Using JMA-Global forecast at 12UTC 3 April 2014 as meteorological field, the 3 days tephra forecast starting at 3.5 hours from the initiation of eruption is computed by JMA-GATM. Under this condition, the tephra particles are transported by the mid-tropospheric southwest wind and widely deposited in Japan. The simulation results show the tephra fall deposits of 10 cm in Hokkaido, which is consistent with the geological survey of Aso-4 tephra. In addition, we performed a parametric study of meteorological field with the same initial distribution of tephra. The simulation results indicate that the depositional pattern of fallout largely depends on the meteorological field. In some cases, the most of the tephra particles are settled not on the land in Japan but on the Pacific Ocean.

Keywords: Atmospheric Transport Model, ignimbrite eruption, tephra, tephra fall, numerical simulation

Japan Geoscience Union Meeting 2015
(May 24th - 28th at Makuhari, Chiba, Japan)

SVC46-P18 Room:Convention Hall Time:May 25 18:15-19:30

Quasi-Realtime Contents of the Tephra Fall Simulations against Large-Scale Eruption

SHIMBORI, Toshiki[1*] ; ISHII, Kensuke[1] ; SATO, Eiichi[1] ; FUKUI, Keiichi[1] ; YOKOYAMA, Hirofumi[1]

[1]Meteorological Research Institute

From FY2014, the Meteorological Research Institute (MRI) of the Japan Meteorological Agency (JMA) is working on research of immediate monitoring and accurate prediction of volcanic phenomena caused by large-scale eruption. Target of the large-scale eruption is the domestic volcano with the volume of ejecta on the order of 10^9 m^3, however, such large-scale eruption has not occurred over the past century. Therefore it is important to simulate the tephra fall against a large-scale eruption in day-to-day weather conditions, from the point of view of roughly predicting the affected area, and also checking and improving the numerical model. For these purposes, assuming the large-scale eruption at Fuji volcano in 1707 (VSJ2013, **P45**) or Sakurajima volcano in 1914 (JpGU2014, **SVC50-P01**), the Volcanology Research Department of the MRI has made the quasi-realtime Internet contents of the large-scale tephra fall predictions with the JMA Regional Atmospheric Transport Model (RATM) driven by the most recent grid point values of the Mesoscale Analysis.

In this presentation, we will introduce the contents planned to daily update on the MRI website.

Keywords: Atmospheric Transport Model, large-scale eruption, volcanic ash, tephra fall, quasi-realtime, numerical simulation

Japan Geoscience Union Meeting 2015
(May 24th - 28th at Makuhari, Chiba, Japan)

SVC46-P19 Room:Convention Hall Time:May 25 18:15-19:30

Numerical assessment of the potential for future limnic eruptions in Cameroon, based on regular monitoring data

KOZONO, Tomofumi[1*] ; KUSAKABE, Minoru[2] ; YOSHIDA, Yutaka[3] ; NTCHANTCHO, Romaric[4] ; OHBA, Takeshi[5] ; TANYILEKE, Gregory[4] ; HELL, Joseph V.[4]

[1]Science, Tohoku Univ., [2]Science, Univ. of Toyama, [3]Yoshida Cons. Eng. Office, [4]IRGM, [5]Science, Tokai Univ.

A limnic eruption is a gas outburst from a lake, and it can cause a catastrophic disaster in the surrounding area. Lakes Nyos and Monoun in Cameroon, Central Africa, are volcanic crater lakes where limnic eruptions with catastrophic releases of CO_2 gas occurred in 1986 (Nyos) and 1984 (Monoun), claiming close to 1800 lives. To understand the mechanism of the limnic eruptions in these lakes, regular monitoring of the chemical composition of the lake water has been conducted since the limnic eruptions, and it allows us to obtain detailed information about CO_2 profiles in the lakes. In this study, we assessed their eruptive potential at Lakes Nyos and Monoun, on the basis of numerical modeling and the CO_2 profiles obtained by the regular monitoring of the lakes.

The evolution of the CO_2 profiles suggests one particular scenario for producing an eruption: supply of CO_2-undersaturated fluid from the lake bottom that induces upwards growth of the bottom layer, leading eventually to CO_2-saturation at mid-depths of the lake. By using a numerical model for the ascent of a plume of CO_2 bubbles, we investigated whether bubble formation in this scenario leads to a bubble plume reaching the lake surface (i.e., a limnic eruption). We found that under realistic conditions (e.g., a CO_2 profile deduced from the regular monitoring data), a bubble plume generated from mid-depths can reach the lake surface with a CO_2 high flux, which corresponds to a limnic eruption. This indicates that the ascent of the bubble plume caused by the upward growth of the CO_2-undersaturated layer is a possible mechanism for inducing a limnic eruption.

Another important factor that affects the current CO_2 profiles in Lakes Nyos and Monoun is the artificial removal of dissolved CO_2 (“controlled degassing”) using degassing pipes. As CO_2-rich water is withdrawn from the deep layer through a pipe, the pipe flow becomes self-sustaining due to bubble formation and expansion caused by decompression in the rising water column. This leads to the formation of a fountain on the lake surface. The most recent CO_2 profiles obtained by the regular monitoring indicate a drastic decrease in the CO_2 concentration at the bottom of the lake. We developed a numerical model for degassing pipe flow so that we could investigate the effects of changes in CO_2 concentration at the lake bottom on the dynamics of the pipe flow and the degree of degassing. From the model, the quantitative relationship between CO_2 concentration at the lake bottom and fountain height observed on the surface of the lake is established. Our results agree well with the observed heights, indicating that our model is successful in capturing the dynamics of the degassing pipe flow in Lakes Nyos and Monoun.

Keywords: Limnic eruption, Lake Nyos, Lake Monoun, Numerical model, Degassing pipe